IOP Conf. Series: Materials Science and Engineering **140** (2016) 012022 doi:10.1088/1757-899X/140/1/012022

Numerical analysis of initial stage of thermal shock

V N Demidov
Tomsk Polytechnic University

E-mail: vn_demidov@mail.ru

Abstract. The paper studies a problem of a thermal shock at the surface of a half-space, which properties are described by elastic-plastic model taking into account dynamic effects, heat inertia, coupling between thermal and mechanical fields. The problem is solved numerically using finite-difference method of S.K. Godunov.

1. Introduction

Numerous advanced technological processes (plasma deposition of coatings, surface treatment by laser or electron-beams, welding, surfacing, etc.) are connected with intense heat impact on a material under treatment. In this case, an abrupt temperature change of the surface occurs, which is termed as thermal shock. Various authors have discussed the role of thermal stresses in stereolithography and in selective laser sintering. A wide group of applied problems is connected with thermal shock problem to a greater or lesser extent [1-2].

The thermal shock problem was originally studied in [3] in terms of so-called theory of thermal stresses [4, 5]. This is the simplest problem formulation enabling analytical solution. Further initial problem formulation has been generalized in several directions, which was noted in reviews [6-8].

In this work, the thermal shock problem was analyzed in generalized formulation taking into account the coupling between thermal and mechanical processes. Here, the interrelation between effects is stipulated by (1) thermal conductivity, (2) dynamical (inertia) terms included in motion equations, (3) coupling between the fields strains and temperature, (4) heat inertia caused by finite rate of heat propagation and (5) dissipative effects due to plasticity. This is one of general formulations of the thermal shock problem.

2. Basic equations of the model

The problem is studied in terms of continuum mechanics. Mathematical model includes the balance equations (mass, impulse, energy):

$$\frac{\partial \rho}{\partial t} + \nabla_m (\rho u_m) = 0, \tag{1}$$

$$\frac{\partial (\rho u_k)}{\partial t} + \nabla_m (\rho u_k u_m - \sigma_{km}) = 0, \quad k = 1,2,3, \tag{2}$$

$$\rho c_\varepsilon \left(\frac{\partial T}{\partial t} + u_m \nabla_m T \right) = -\nabla_m q_m - 3K\alpha T \nabla_m u_m + s_{km} e^p_{km}, \tag{3}$$

and constitutive equations for heat flux vector:

$$q_k + \tau_q\left(\frac{\partial q_k}{\partial t} + u_m \nabla_m q_k\right) = -\lambda \nabla_k T, \quad k = 1,2,3, \tag{4}$$

and stress tensor

$$\frac{\partial s_{ik}}{\partial t} + u_m \nabla_m s_{ik} - \omega_{im} s_{km} - \omega_{km} s_{im} + \Lambda s_{ik} = 2\mu e_{ik}, \quad k = 1,2,3, \tag{5}$$

$$p = p(\rho, T), \tag{6}$$

where

$$\varepsilon_{ik} = \varepsilon_{ik}^e + \varepsilon_{ik}^p, \quad \varepsilon_{ik} = \tfrac{1}{2}(\nabla_i u_k + \nabla_k u_i), \quad e_{ik} = \varepsilon_{ik} - \tfrac{1}{3}(\nabla_m u_m)\delta_{ik},$$
$$\omega_{ik} = \tfrac{1}{2}(\nabla_k u_i - \nabla_i u_k), \quad \sigma_{ik} = -p\delta_{ik} + s_{ik}, \quad p = -\tfrac{1}{3}\sigma_{km}\delta_{km},$$
$$s_{km}s_{km} \le \tfrac{2}{3}\sigma_Y^2, \quad \Lambda = \frac{3\mu s_{km} e_{km}^p}{\sigma_Y^2} H\left(s_{km}s_{km} - \tfrac{2}{3}\sigma_Y^2\right) H\left(s_{km}e_{km}^p\right).$$

Here ρ is density, $\sigma_{ik}, \varepsilon_{ik}, \delta_{ik}$ are components of the stress tensor, strain rate tensor and identity tensor, respectively, u_k are the components of velocity vector, T is temperature, c_ε is the thermal capacity at constant strains, α is linear thermal expansion coefficient, λ is thermal conductivity coefficient, K is isothermal bulk module, τ_q is the relaxation time for heat flux, μ is shear module, σ_Y is dynamic yield point, H is Heaviside function.

Individual terms in the right part of the equation (3) describe the dissipation due to thermal conductivity ($\nabla_m q_m$), coupling between thermal and deformation processes ($3KT\alpha_T \nabla_k u_k$) and irreversible effects caused by plastic flow ($s_{km}e_{km}^p$). Here, it is supposed that stress work with plastic strains disperses completely turning into heat.

The structure of relation (4), which is usually called as the generalized Fourier's law, is identical to that of the Maxwell relaxation equation. This equation can be obtained formally by adding term $\tau_q dq/dt$ to the classical Fourier's law of thermal conductivity $q_k = -\lambda \nabla_k T$ which accounts for heat inertia. From the physical point of view, the difference between (4) and classical Fourier's law is that the generalized law takes into account a *delay effect* conditioned by the relaxation of the system to the thermodynamic equilibrium. Equation (4) can be interpreted as the generalization of Onsager relations for the case of disturbed local thermodynamic equilibrium in the fields of large (infinite) gradients of temperature field under a thermal shock. From the other hand, it can be construed as a particular case of the state equation with thermal memory [9].

Equation (5) connecting the deviators of stress tensor s_{ik} and strain rate tensor e_{ik} can be obtained with the assumption of the hypoelastic deformation law for elastic component e_{ik}^e in the additive decomposition $e_{ik} = e_{ik}^e + e_{ik}^p$ (in the hypoelastic deformation law, the Jaumann derivative is assumed as the objective measure for the rate of the stress field change), and with the assumption of the associated flow rule with von Mises plasticity condition for the plastic component e_{ik}^p.

Equation (6) is the thermal state equation for spherical stress tensor (p is hydrostatic pressure).

3. Problem formulation

Let us examine the elastic plastic half-space $x \equiv x_1 \ge 0$, surface temperature of which grows instantly from T_0 to T_b at initial time moment $t = 0$ and then stays constant, i.e.

$$T\big|_{x=0} = T_b H(t) \tag{7}$$

The present work studies the initial wave stage of half-space motion initiated by external heat action (7). Here, we analyze two types of mechanical boundary conditions: the plane $x = 0$ is free of stresses (problem I)

$$\sigma_{11}\big|_{x=0} = \sigma_{12}\big|_{x=0} = \sigma_{13}\big|_{x=0} = 0, \tag{8}$$

and the plane $x = 0$ is rigidly fixed (problem II)

$$u_1\big|_{x=0} = u_2\big|_{x=0} = u_3\big|_{x=0} = 0 \tag{9}$$

Initial conditions

$$\sigma_{ik}\big|_{t=0} = \varepsilon_{ik}\big|_{t=0} = u_k\big|_{t=0} = 0, \quad T\big|_{t=0} = T_0, \quad \rho\big|_{t=0} = \rho_0 \tag{10}$$

correspond to not stressed and not deformed quiescent half-space with uniform initial temperature and density.

Due to the uniformity of initial and boundary conditions, both problems are one-dimensional; in the half-space, a one-axis strain state is realized; hence, the following assumptions should be made for system of equations (1)–(5):

$$u_2 = u_3 = 0, \quad q_2 = q_3 = 0, \quad \varepsilon_{11} = \frac{\partial u_1}{\partial x}, \quad \varepsilon_{22} = \varepsilon_{33} = 0, \quad \varepsilon_{ik} = 0,\ i \neq k,$$

$$e_{11} = \frac{2}{3}\frac{\partial u_1}{\partial x}, \quad e_{22} = e_{33} = -\frac{1}{3}\frac{\partial u_1}{\partial x}, \quad \sigma_{ik} = 0,\ i \neq k, \quad s_{22} = s_{33} = -\frac{1}{2}s_{11}.$$

4. Calculation results

We assume that material is steel with the following properties:

$$c_\varepsilon = 498\ \mathrm{J/(kg \cdot K)}, \quad K = 162.1\ \mathrm{GPa}, \quad \alpha_T = 10^{-6}\ \mathrm{K^{-1}}, \quad \lambda = 80\ \mathrm{W/(m \cdot K)},$$

$$\mu = 90.6\ \mathrm{GPa}., \quad \tau_q = 10^{-11}\mathrm{s}, \quad \sigma_Y = 0.75\ \mathrm{GPa}, \quad \rho_0 = 7.85\ \mathrm{g/cm^3}.$$

Initial and boundary temperature are $T_0 = 293\ \mathrm{K}$ and $T_b = T_0 + 1000\ \mathrm{K}$, respectively. Numerical results were obtained using the difference scheme of Godunov S.K. [10]. It is a uniform monotonic scheme with first-order accuracy; its inherent properties are similar to known gas-dynamic Godunov's scheme [11].

The results are shown in Figures 1–6. In all figures, the profiles of physical parameters corresponding to problem I are shown with thick (blue) lines; and profiles corresponding to problem II are shown with thin (dark) lines. The numbers near the curves correspond to different moments of dimensionless time $t' = t / \tau_q$, where the scale is determined by the relaxation time of heat flux. Additionally, the dotted lines in Figure 4 give the temperature for the solution of parabolic thermal conductivity equation

$$T(x,t) = (T_b - T_0)\,erfc\left(\frac{x}{2\sqrt{at}}\right), \qquad a = \frac{\lambda}{\rho c_\varepsilon}, \tag{11}$$

and dot-and-dash lines illustrate the solution of hyperbolic thermal conductivity equation [9]:

$$T(t,x)=T_0+H\left(t-\frac{x}{a_T^2}\right)\left\{T_b\,exp\left(-\frac{x}{2a_T\tau_q}\right)+\right.$$
$$\left.+\frac{x}{2a_T\tau_q}\int_0^x\frac{T_b}{\sqrt{(t-\eta)^2-x^2a_T^{-2}}}I_1\left(\frac{\sqrt{(t-\eta)^2-x^2a_T^{-2}}}{2\tau_q}\right)exp\left(-\frac{t-\eta}{2\tau_q}\right)d\eta\right\}, \quad (12)$$

where $a_T=\sqrt{a\tau_q^{-1}}$, I_1 is a modified Bessel function of first kind, H is the Heaviside function.

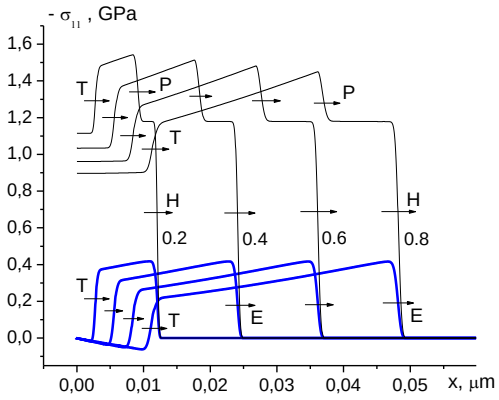

a

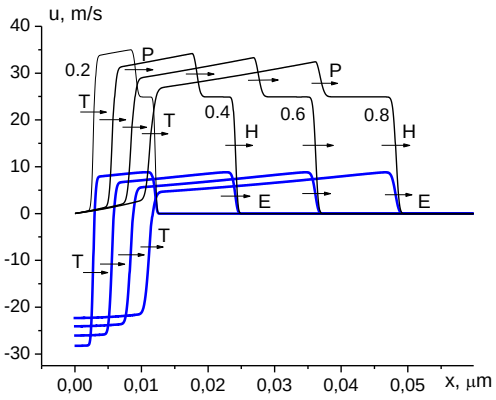

a

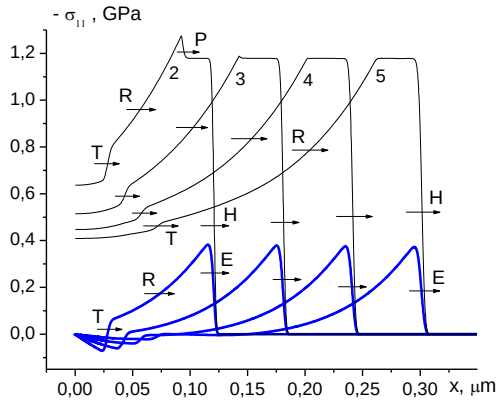

b

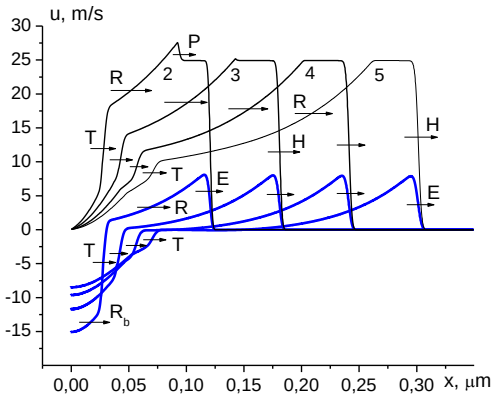

b

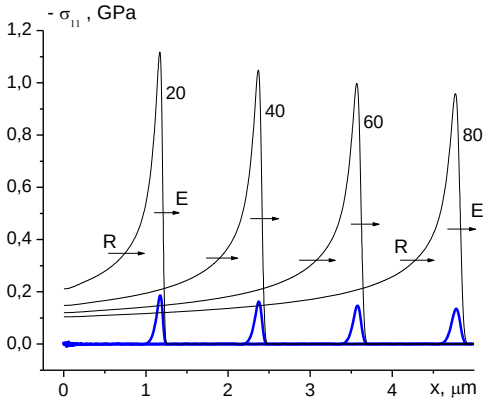

c

Figure 1. Stress profiles for sequential time moments. Time intervals: a) 0–1 s; b) 1–10 s; c) 10–100 s.

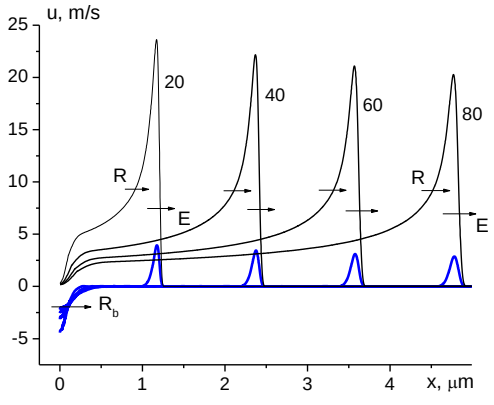

c

Figure 2. Velocity profiles for sequential time moments. Time intervals: a) 0–1 s; b) 1–10 s; c) 10–100 s.

Let us consider the qualitative features of the wave picture of motion developing at the initial stage of thermal shock.

First of all, we should note that there are several different velocities for the propagation of thermomechanical perturbations. Taking into account the coupling of heat and deformation processes, the propagation rates for quick a_1 and slow a_2 waves can be presented as [10]:

$$a_{1,2} = \sqrt{\tfrac{1}{2}\left(a_E^2 + a_T^2\right) \pm \tfrac{1}{2}\sqrt{\left(a_E^2 - a_T^2\right)^2 + 4T\left(3K\alpha a_T\right)^2 c_\varepsilon^{-1}\rho^{-2}}}\,, \tag{13}$$

where the value of $a_E = \sqrt{\left(K_S + 4\mu/3\right)\rho^{-1}}$ corresponds to the propagation velocity of longitudinal elastic waves, and $a_T = \sqrt{a/\tau_q}$ is the thermal wave velocity for the case when coupling effects are omitted. Here K_S is adiabatic bulk module, $a = \lambda\left(\rho c_\varepsilon\right)^{-1}$ is thermal diffusivity coefficient. In addition, there are still two velocities, $a_H \approx a_E$ and $a_P \approx \sqrt{K_S/\rho}$; a_H correspond to the velocity of elastic predecessor, a_P is the plastic wave velocity.

As a rule, the coupling coefficient for metals is small [4, 9]. When we neglect this effect and remove the last term from formula (13), the approximate equalities can be written as

$$a_1 \approx a_E \approx a_H\,, \qquad a_2 \approx a_T\,.$$

In the case under study, $a_H \approx a_E = 6022$ m/s, $a_P = 4569$ m/s, $a_T = 1431$ m/s.

According to above, elastic-plastic wave initiated by thermal shock, has several specific parts. For convenience, we will term the waves propagating with velocities a_E, a_H, a_P, a_T as E-, H-, P-, and T-waves, respectively. Figures. 1–4 show that the state of medium alters in these waves unevenly. The sharp growth in temperature and pressure occurs in the front of T-wave. Behind this wave, the intense expansion of the substance is observed that leads to the formation of the impulse of tensile stresses in problem I (Figure 1), and the motion velocity of free surface in the negative direction of x-axis is tens meters per second (Figure 2). The processes developing in the T-wave has fierce irreversible character which is obvious from the pressure profiles (Figure 3): first, "over-compressing" occurs, than "over-expansion" of the substance emerges, and only at $t \sim 10\tau_q$ the pressure limits to a reversible value ($p =$ 0.5 GPa) corresponding to the regime determined by boundary conditions ($\sigma_{11} \equiv s_{11} - p = 0$).

The region of continuous flow lies between E- and T-waves; it corresponds to the unloading wave, marked in the figures by letter R. With time, this wave decreases the stress to zero; further, T- and E-waves look as separated in problem I (Figures. 1–3, $t' = 20-80$). However, the interrelation between them persists, and the processes developing in T-wave affect appreciably E-wave attenuation.

Quantitative difference in the solutions of problems I and II, shown clearly in Figures. 1–3, are evidently connected with the condition of hindered deformation in problem II. The material of the half-space having endured a large volume expansion behind T-wave, cannot expand freely in the negative direction of x-axis due to the fixation condition. As a result, the pressure behind T-wave in problem II is higher than that in problem I, and stress σ_{11} stays compressive. In addition, the adjugate P-jump appears in problem I. It is connected with the intensity of tangential stresses behind H-wave reaching maximum possible value corresponding to the von Mises yield condition. Stress σ_{11} in H-wave equals to Hugoniot elastic limit on shock adiabat. The adiabat has a kink in this point, and the stress exceeding the Hugoniot limit propagates with the volume wave velocity a_P.

Figure 4 shows that for small times, the numerical solution agrees well with the analytical solution of hyperbolic thermal conductivity equation (12), and for large times, with the solution of parabolic equation (11). For any time, the contribution of mechanical effects to temperature field can be ignored. Negligibly small effect of elastic plastic strains in the temperature change is shown in Figure 5. Elastic wave of limiting intensity, H-wave, increases the temperature for 1.5 degrees.

The stress profiles $\sigma_{11}(x)$ are presented in Figure 6 for three time moments $t' = 0.1, 0.2, 0.3$ seconds (problem I).

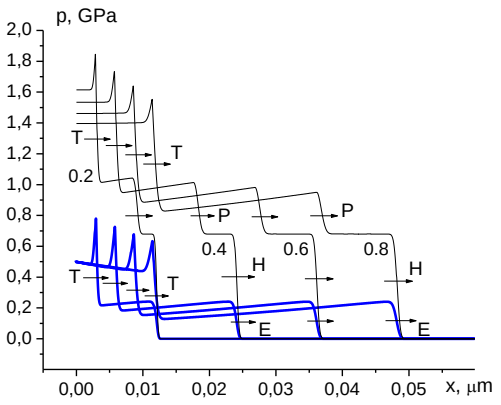

a

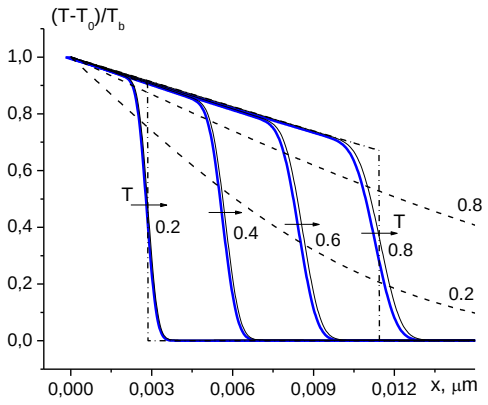

a

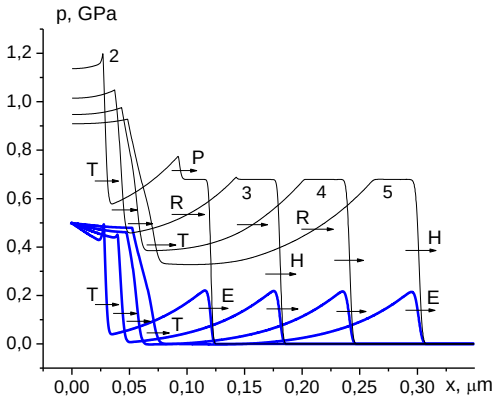

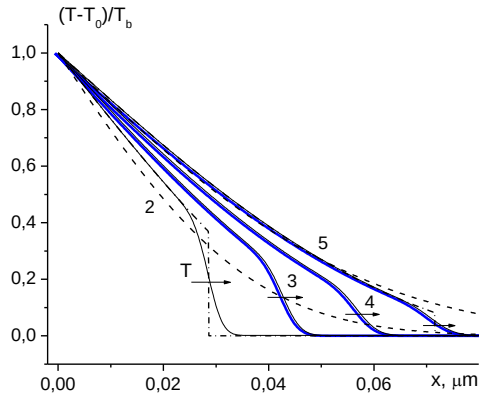

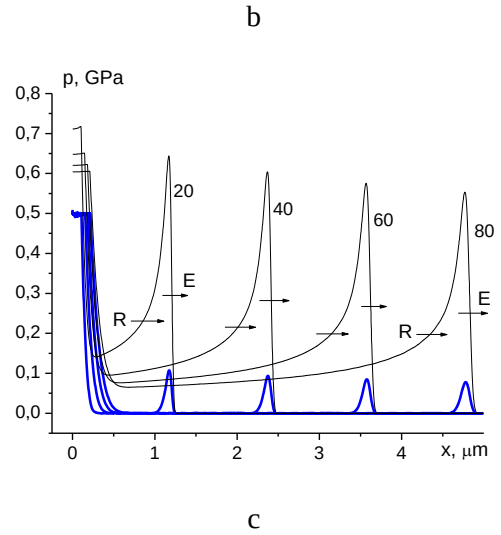

Figure 3. Pressure profiles for sequential time moments. Time intervals: a) 0–1 s; b) 1–10 s; c) 10–100 s.

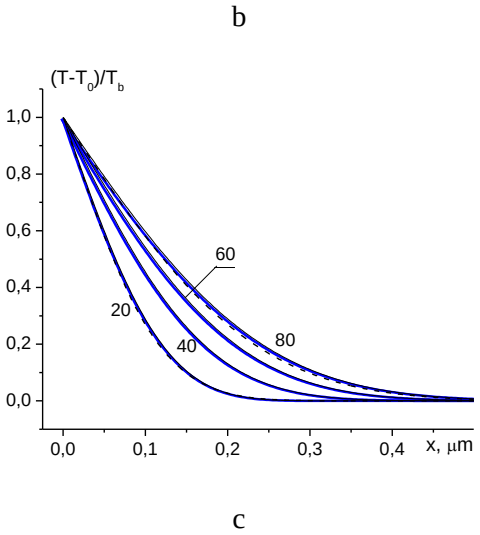

Figure 4. Temperature profiles for sequential time moments. Time intervals: a) 0–1 s; b) 1–10 s; c) 10–100 s.

The known thermoelastic solution [12]

$$\sigma_{11}(x,t) = -A\left[D(x,t) + E(x,t)\right], \tag{14}$$

where

$$A = 3K_T\alpha_T\left(T_b - T_0\right), \quad E(x,t) = \frac{1}{2}exp\left[\frac{a_E^2}{a}\left(t - \frac{x}{a_E}\right)\right]H\left(t - \frac{x}{a_E}\right)$$

$$D(x,t) = \frac{1}{2}exp\left[\frac{a_E^2}{a}\left(t + \frac{x}{a_E}\right)\right]erfc\left(\frac{x}{2\sqrt{at}} + a_E\sqrt{\frac{t}{a}}\right) + \frac{1}{2}exp\left[\frac{a_E^2}{a}\left(t - \frac{x}{a_E}\right)\right]erfc\left(\frac{x}{2\sqrt{at}} - a_E\sqrt{\frac{t}{a}}\right),$$

is also shown here for the same times for the sake of comparison.

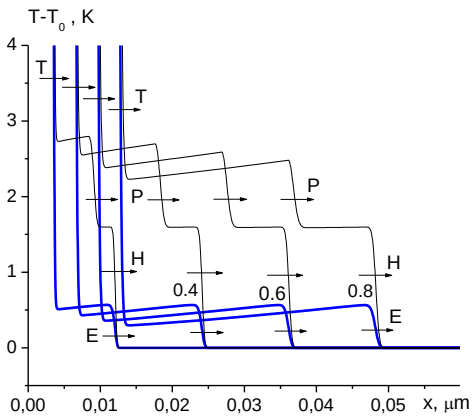

Figure 5. Temperature profiles for sequential time moments

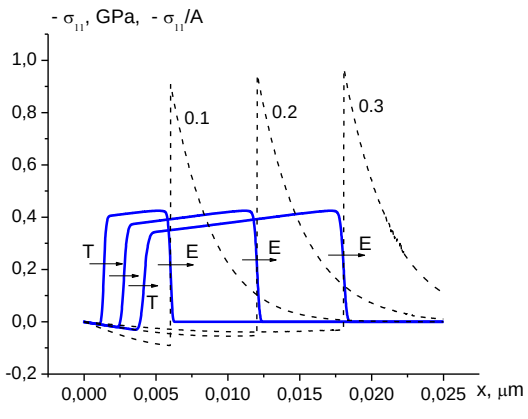

Figure 6. Stress profiles for sequential time moments. Comparison with classical thermoelastic solution (dotted line).

Diffusion part of the problem described by function $D(x,t)$ corresponds to infinite velocity of heat propagation; hence, compressive stresses appear immediately in each point of the half-space. The second term $E(x,t)$ determines the elastic wave $E(x,t)$ propagating with velocity a_E. Stress σ_{11} changes unevenly by value A in the front of this wave (in the example under study, $A = 4.86$ GPa) and turns tensile. The solution described by equation (14) does not even qualitatively conform with the solution obtained in this work. Quantitative comparison is useless because the solution (14) is correct, if the condition $(T - T_0)T_0^{-1} << 1$ was satisfied, which is not in considered case.

5. Conclusion

The problem of thermal shock is studied here for the half-space with the properties described by an elastic plastic model taking into account dynamical effects, heat inertia, coupling between heat and mechanical fields. The problem was solved numerically using S.K. Godunov's method.

The obtained results show that wave picture accompanying a thermal shock is incomparably richer and more complex, as compared to those predicted by known thermoelastic solutions.

In this connection, we note that the evaluations of the thermal strength of materials based on the solutions of type (14) used in the literature can be inconsistent, because the fracture of surface layers, if any, develops at the initial (wave) stage of thermal shock, when the relative role of the factors connected with mechanical and heat inertia is maximal and actually determines the following evolution of a thermal stresses field. Therefore, residual stresses under local thermal action do not correspond to the solutions of quasistatic problems [13].

Results obtained for the heat part of the problem once more corroborate the known situation about weak influence of the coupling effect on temperature distribution. On all occasions, this is correct for typical construction materials and alloys on the basis of iron and aluminum. For these materials, one can neglect the contribution of mechanical processes to temperature field and use the hyperbolic equation (for $t \le 10\tau_q$) or more simple parabolic thermal conductivity equation (for $t \ge 100\tau_q$). However, the relative contribution of plastic strains for nonmetallic materials can appreciably different in comparison with the example studied here.

In conclusion we should note that the thermomechanical wave attenuation is strongly affected by all the factors named in the initial part of the paper (dynamic effects, heat inertia, coupling) and by boundary conditions determined for the free surface of a half-space.

Acknowledgments

This work was supported by the Ministry of Science and Education of the RF, project No. 11.815.2014/K.

References

[1] Rykalin N N, Zuev A A and Uglov A A 1978 *The foundation of electron-beam treatment of materials (in Russian)* (Moscow: Mashinostroenie) p 239

[2] Lawrence E Murr, Sara M Gaytan, Diana A Ramirezb, Edwin Martinez, Jennifer Hernandez, Krista N Amato, Patrick W Shindo, Francisco R Medina and Ryan B 2012 Wicker Metal Fabrication by Additive Manufacturing Using Laser and Electron Beam Melting Technologies *J. Mat. Sc. & Tech.* **28 1** 1–14

[3] Danilovskaya V I 1950 Thermal Stresses in an Elastic Half-Space Arising After a Sudden Heating of Its Boundary (in Russian) *Prikl. Mat. Mech.* **14 3** 316-318

[4] Boley B A and Weiner I H 1960 *Theory of thermal stresses* (New York: Wiley)

[5] Parkus H 1959 *Instutionäre Wärmespannungen* (Vienna: Springer)

[6] Kartashev E M, Parton V Z 1991 *Dynamic thermoelasticity and problems of thermal shock (in Russian)* (Itogi Nauki I techniki VINITI. Ser. "Mechanics of deformable solid body") **22** 55-127

[7] Xiangmin Zhou 2008 *Journal of Thermal Stresses* **31 7** 663-664

[8] Richard B Hetnarski and Eslami M. Reza 2009 *Thermal Stresses – Advanced Theory and Applications* (Berlin: Springer)
[9] Lykov A V 1978 *Heat and mass transfer. Reference book (in Russian)* (Moscow: Energiya)
[10] Demidov V N 1999 Godunov's Method for generalized one-dimensional dynamical problems of thermal elastic plasticity – *in "Mathematical modelling in synergetic systems". All-Russian scientific conference (Tomsk-Ulan-Ude July, 20-23, 1999)* pp 226-228
[11] Godunov S K 1958 Difference method for the calculation of discontinuous solutions in hydrodynamics (in Russian) *Mathematical collection* **47 3** 271-306.
[12] Nowacki V 1970 *Dynamiczne zagadnienia termosprezystosci. Warshava, (Nowatskii V. Dynamical problems of thermal elasticity (translated to Russian)* (Moscow: Mir) p 250
[13] Burenin1 A A, Dats E P and Murashkin E V 2014 Formation of the Residual Stress Field under Local Thermal Actions *Mechanics of Solids* **49 2** 218–224